Comparison study of electron correlation in one-photon and two-photon double ionization of helium

Wei-Chao Jiang, Liang-You Peng,* Wei-Hao Xiong, and Qihuang Gong
State Key Laboratory for Mesoscopic Physics and Department of Physics, Peking University, Beijing 100871, China
(Received 5 March 2013; published 8 August 2013)

Based on *ab initio* time-dependent calculations for helium, we study the joint angular distribution (JAD) of the two electrons ionized by absorbing one or two photons. On the JAD plane for the equal energy sharing case, one can identify a common symmetric ejection mode with respect to the laser polarization for three different processes, i.e., one-photon double ionization, two-photon nonsequential ionization, and sequential double ionization. In this symmetric ejection case, the two ejected electrons strongly favor a particular interelectron angle. We show that this angle can mimic the electron correlation strength in these double-ionization processes. The interelectron angle in the three types of double ionization is found to be obviously different.

DOI: 10.1103/PhysRevA.88.023410 PACS number(s): 32.80.Rm, 42.50.Hz, 42.65.Re

I. INTRODUCTION

In the past 20 years, electron correlation effects in the double ionization of atoms or molecules have attracted a lot of attention since people realized that the single active approximation is insufficient to explain all the experiment results [1–4]. The technological advances of free electron lasers (FELs) [5–7] and the attosecond pulses [8,9] have brought great opportunity to study the electron correlation in the multiple ionization of atoms or molecules by absorbing a few photons. For the simplest multiple-electron atom of helium, the one-photon double-ionization process seems to have been understood well in both theories and experiments [10,11]. In the late 1990s and the beginning of this century, a large number of experiments were performed to measure two-electrons' angular distributions in the one-photon double-ionization process of helium [12–21], with the excess energy varying from 0.1 eV [12] to 450 eV [13]. These measured distributions coincide with the predictions of theories very well and can be modeled with a simple formula [10,22–24]. As far as we know, there is still no corresponding experiment that measures two electrons' angular distributions in the two-photon double-ionization process of helium, since the signals are much smaller than those in the one-photon case. Nevertheless, a few experiments [25–27] which measured the total cross section of two-photon double ionization of helium have already been performed, which is a good start for future differential measurements.

Different from the situation in experiments, a large number of theoretical studies exist on the topic of two-photon double ionization of helium [28–55]. Angular distributions of the two ejected electrons in two-photon double ionization can be quite different from the situation in one-photon double ionization. For example, it is well known that the ejection mode in which two equal energy sharing electrons are ejected in opposite directions (back-to-back) is forbidden in the one-photon process of helium [10], but such a mode is the most favorable ejection mode in the two-photon process of helium [29,30,37]. This difference comes from the different parities of the final wave function induced by absorbing different numbers of photons [10]. Although many efforts have recently been put into the study of two-photon double ionization, the exact mechanism is still not completely clear [56]. A key question is to what extent the electron correlation plays its role in different ionization processes [50–54]. It is natural to infer that the different strengths of the electron correlation in different ionization processes may lead to different angular distributions of the two ejected electrons. Recently, Feist *et al.* [50] investigated the electron correlation effects from the angular distributions of the two ejected electrons in the two-photon sequential double-ionization process of helium. The motivation of the present study is to carry out a comparative study of the electron correlation effect in different types of double-ionization processes, i.e., one-photon double ionization, two-photon nonsequential ionization, and sequential double ionization.

In this paper, we focus on the joint angular distribution (JAD) of the two ionized electrons for the equal energy sharing case [57]. We identify the common and different features on the distributions for these three types of double ionization. In particular, there exists a common symmetric ejection mode with respect to the laser polarization for all the three cases. In this symmetric mode, the two electrons are ejected in a favorable interelectron angle. We show that this angle is closely related to the electron correlation in the double ionization. In the one-photon case, the angular distribution can be fitted well by a widely known formula [10,22,23]. The interelectron angle defined in the present work is directly related to the fitting parameter, which was previously used to measure the electron correlation [10,19]. For the same excess energy, the interelectron angle in the two-photon nonsequential double ionization is found to be obviously smaller than that in the one-photon double-ionization process and larger than that in the two-photon sequential double-ionization process. The dependence of the interelectron angle on the excess energy also shows quite different behaviors in the one-photon double-ionization process and the two-photon nonsequential double-ionization process. Our results show that the ejection angle mimics the electronic correlation.

The rest of paper is organized as follows. In Sec. II, we briefly describe our theoretical method, which is based on the *ab initio* solution of the two-electron time-dependent Schrödinger equation [57,58]. In Sec. III, we provide our numerical results and discussions. Finally, we make a short conclusion in Sec. IV.

*liangyou.peng@pku.edu.cn

II. THEORETICAL METHOD

In order to get the joint angular distributions of the two ejected electrons, we solve the time-dependent Schrödinger equation (TDSE) numerically in its full dimensionality. The TDSE of helium in a linearly polarized laser field is given by

$$i\frac{\partial}{\partial t}\Psi(\mathbf{r}_1,\mathbf{r}_2,t) = H(t)\Psi(\mathbf{r}_1,\mathbf{r}_2,t), \tag{1}$$

where the Hamiltonian operator, in the dipole approximation and length gauge, can be written as

$$H(\mathbf{r}_1,\mathbf{r}_2,t) = \frac{\mathbf{p}_1^2}{2} + \frac{\mathbf{p}_2^2}{2} - \frac{2}{r_1} - \frac{2}{r_2} + \frac{1}{|\mathbf{r}_1-\mathbf{r}_2|} + (\mathbf{r}_1+\mathbf{r}_2)\cdot\mathbf{E}(t), \tag{2}$$

where $\mathbf{E}(t)$ is the electric field of the laser pulse.

We employ spherical coordinates so as to use the usual close-coupling scheme to treat the angular coordinates analytically. In the close-coupling scheme, the two-electron wave function $\Psi(\mathbf{r}_1,\mathbf{r}_2,t)$ is expanded in coupled spherical harmonics,

$$\Psi(\mathbf{r}_1,\mathbf{r}_2,t) = \sum_{L,M,l_1,l_2} \frac{R^{L,M}_{l_1,l_2}(r_1,r_2,t)}{r_1 r_2} Y^{L,M}_{l_1,l_2}(\hat{r}_1,\hat{r}_2), \tag{3}$$

in which

$$Y^{L,M}_{l_1,l_2}(\hat{r}_1,\hat{r}_2) = \sum_{m_1,m_2} \langle l_1 m_1 l_2 m_2 | l_1 l_2 L M\rangle \times Y_{l_1,m_1}(\hat{r}_1) Y_{l_2,m_2}(\hat{r}_2), \tag{4}$$

where $\langle l_1 m_1 l_2 m_2 | l_1 l_2 L M\rangle$ is the usual Clebsch-Gordan coefficient.

Substitution of Eq. (3) into Eq. (1) leads to a set of coupled equations for the radial wave function $R^{L,M}_{l_1,l_2}(r_1,r_2,t)$, which is discretized using the normalized Gauss-Lobatto finite-element discrete variable representation (FEM-DVR) basis functions [59,60], whose advantages, detailed in Ref. [57], have been previously demonstrated by many other authors [61–63]. The matrix elements of the electron-electron Coulomb repulsion term in the Hamiltonian need to be handled especially carefully; we follow the treatment reviewed by McCurdy *et al.* [64]. The propagation of the time-dependent wave function is obtained using an effective iterative Arnoldi-Lanczos method [65], whose accuracy and stability have been verified in a number of recent works [29,37,66,67]. For technical details of the numerical methods, we refer the readers to the above references.

Here we only give the typical calculation parameters used for the present study. The radial coordinates of the two electrons are truncated at $r_{i,\max} = 200$ a.u., where $i = 1,2$. Each radial coordinate is discretized by using 105 finite elements (FEM) and 8 Gauss-Lobatto quadrature points on each element. For the angular coordinates, the close-coupling expansion is truncated at $l_1 = l_2 = 5$ and $L = 3$, where l_1 and l_2 are, respectively, the quantum number of the angular momentum of each electron and L is the quantum number of the total angular momentum of the two electrons. Please note that $M = 0$ for a linearly polarized laser. Typically, the wave function is further propagated freely for a time about 20–30 a.u. after the end of the laser pulse. Once the final wave function $\Psi(\mathbf{r_1},\mathbf{r_2})$ is computed, we project it to the double-ionization continuum, which is approximated by the product of two Coulomb waves $\phi_{\mathbf{k}}(\mathbf{r})$ with the nuclear charge $Z = 2$, to get the differential probability density:

$$P(E_1,E_2,\theta_1,\theta_2,\varphi_1,\varphi_2) = \left|\langle\phi_{\mathbf{k_1}}(\mathbf{r_1})\phi_{\mathbf{k_2}}(\mathbf{r_2})|\Psi(\mathbf{r_1},\mathbf{r_2})\rangle\right|^2, \tag{5}$$

where $E_1 = k_1^2/2$ and $E_2 = k_2^2/2$. Note that the laser is assumed to be polarized along the z axis and the electron emission angles are defined with respect to this axis. In this study, we focus only on the case where the two electrons share the same excess energy ($E_1 = E_2 = E_{\rm exce}/2$, $E_{\rm exce} = n\hbar\omega - I_p$, and $I_p \approx 79.01$ eV) and are ejected on the coplane of $\varphi_1 = \varphi_2 = 0$ or π.

In most of the following calculations, we assume the vector potential of the laser pulse has a sin-square envelope:

$$\mathbf{A}(t) = \mathbf{A}_0 \cos^2\left(\frac{\pi t}{T}\right)\sin(\omega t), \tag{6}$$

where T is the total pulse duration and ω is the center frequency (or photon energy). The electric field strength is given by $\mathbf{E}(t) = -\frac{\partial \mathbf{A}(t)}{\partial t}$. We use a sufficiently long pulse so that the interelectron angle, of which quantity we focus on in the present work, does not change significantly upon further increase of T. We also note that the usage of pulse shape other than sin square does not change our main results.

III. NUMERICAL RESULTS

In this section, we present our main results. In Sec. III A, we look at the joint angular distribution of the two electrons and identify the different features for these three types of double-ionization processes. Then in Sec. III B, we focus on the common features on the diagonal line of $\theta_1 + \theta_2 = 2\pi$, which represents the symmetric ejection mode of the two electrons with respect to the laser polarization in the same hemisphere. We then clearly define the interelectron angle, followed by a detailed study for the one-photon double-ionization case. We establish a direct link between the interelectron angle and the parameter previously used to measure the electron correlation in the literature. In Sec. III C, we carry out systematic and comparative study of the interelectron angle for the three types of double-ionization processes, as a function of the excess energy $E_{\rm exce}$. These studies show that the interelectron angle can well mimic the electron correlation.

A. Different features in JAD

In this subsection, we discuss the different features exhibited in the joint angular distributions for the three types of double ionization. Different from the one-photon double-ionization process, where the two electrons have to be ejected at nearly the same time, in the two-photon double-ionization process the two electrons are allowed to be ejected one by one by absorbing one photon separately, depending on the photon energy. For long enough pulses, the two-photon double-ionization process can be distinguished as two quite different types according to energies of the two photons (ω_1 and ω_2): in the sequential double-ionization case where $\omega_1 > 24.6$ eV, $\omega_2 > 54.4$ eV, $\omega_1 \leqslant \omega_2$, and $\omega_1 + \omega_2 > 79.01$ eV, it is allowed that the first electron is ionized by absorbing a photon ω_1 and

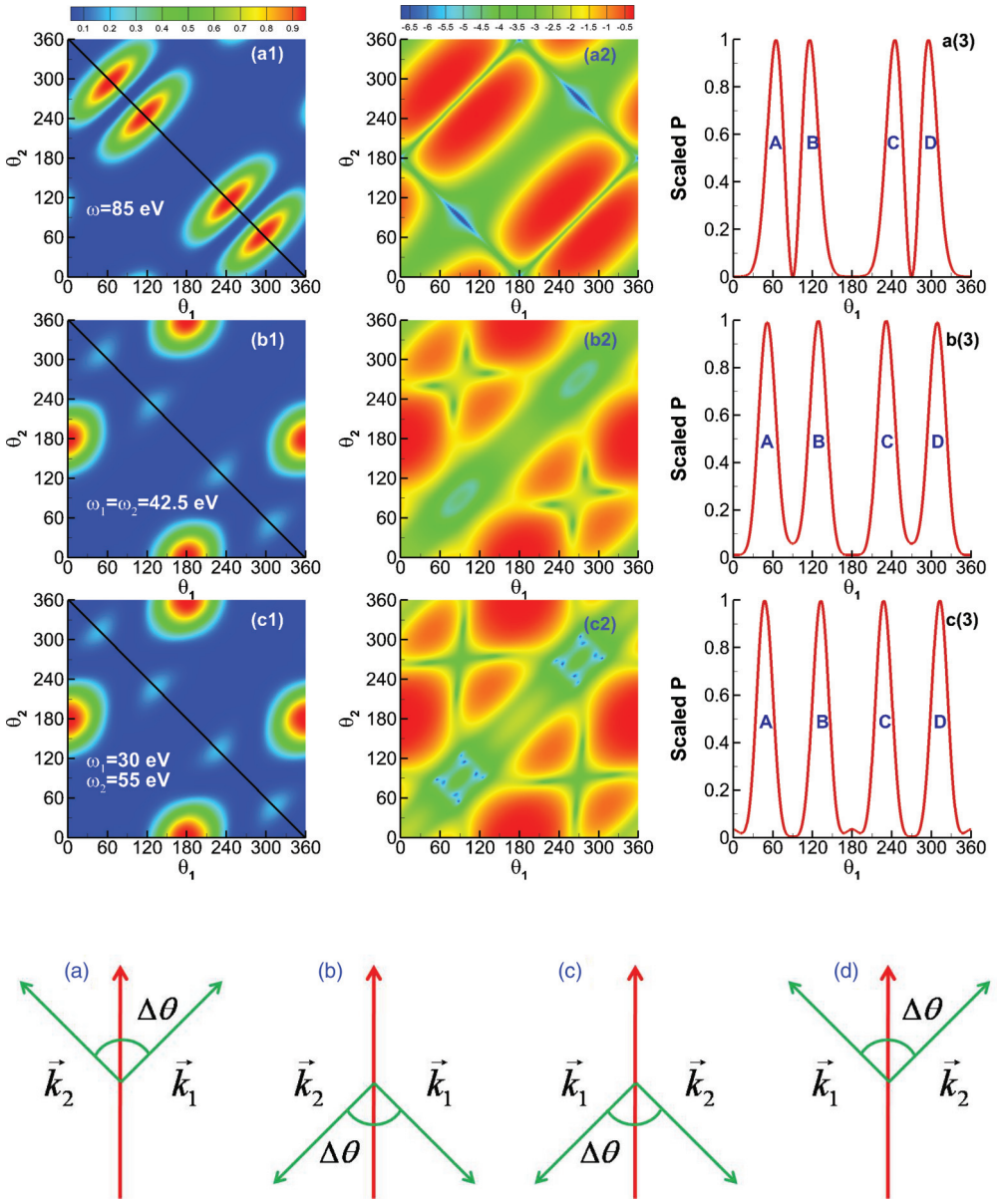

FIG. 1. (Color online) The coplanar angular distributions of the two equal energy sharing electrons for the one-photon double-ionization process (the first row), the two-photon nonsequential double-ionization process (the second row), and the two-photon sequential double-ionization process (the third row). The photon energies are marked in each panel of the first column, in which the differential probability density is shown in the same normalized linear scale. The second column shows the corresponding differential probability density on the same normalized log scale. The third column shows the scaled differential probability along the line $\theta_1 + \theta_2 = 360^\circ$, which is marked as a black line in each panel of the first column. The data in the third column have been scaled to unit at the maxima value for clarity. The four peaks (marked as A, B, C, and D) are illustrated with sketched maps in the bottom row.

then the second electron is ionized by absorbing a photon ω_2; in the nonsequential double-ionization case where $\omega_1 \leqslant \omega_2 < 54.4$ eV and $\omega_1 + \omega_2 > 79.01$ eV, the two electrons have to be ionized by absorbing the two photons at almost the same time since the sequential process is energetically forbidden and the electron correlation must play an essential role.

The three ionization processes, one-photon double ionization, two-photon nonsequential double ionization, and two-photon sequential double ionization, will produce different features in energy spectra, which have been widely discussed previously [29,30,37,40]. To show the different and common features in the joint angular distributions of the two electrons in the three processes, we present in Fig. 1 typical distributions for each process on the coplane of $\varphi_1 = \varphi_2 = 0$ or π in the equal energy sharing case. Similar joint angular distributions for two-photon processes have been discussed in Ref. [57], where the integration over the electron energy has been carried out. However, in Fig. 1, we show the full differential probability distribution. For the one-photon double ionization, as can be most clearly seen from Fig. 1(a2), the back-to-back ejection mode (i.e., $\theta_1 - \theta_2 = \pm\pi$) is forbidden [10]. Another forbidden ejection mode for the one-photon double ionization

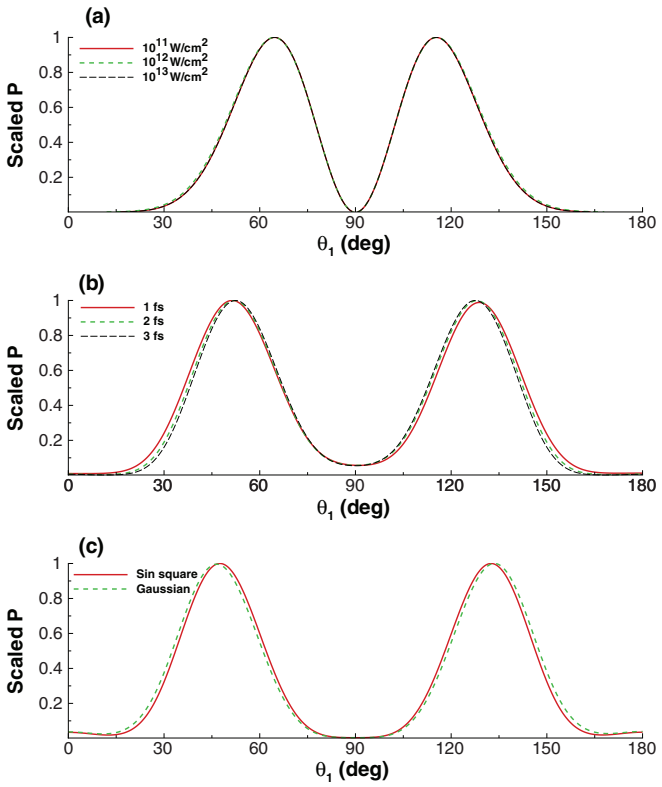

FIG. 2. (Color online) Insensitivity of angular distribution shapes along the line of $\theta_1 + \theta_2 = 360^\circ$ on the pulse intensity (a) and the pulse length (b). In panel (a), results are shown for three different intensities for the one-photon double ionization at a photon energy of 85 eV and a pulse duration of 15 cycles. In panel (b), results are shown for two-photon nonsequential double ionization for three different pulse durations at a photon energy of 42.5 eV and a peak intensity of 10^{12} W/cm^2. In panel (c), results are shown for two-photon sequential double ionization for two different pulse shapes (sin square and Gaussian) at photon energies of 30 and 55 eV, a peak intensity of 10^{12} W/cm^2, and a pulse duration of 3 fs.

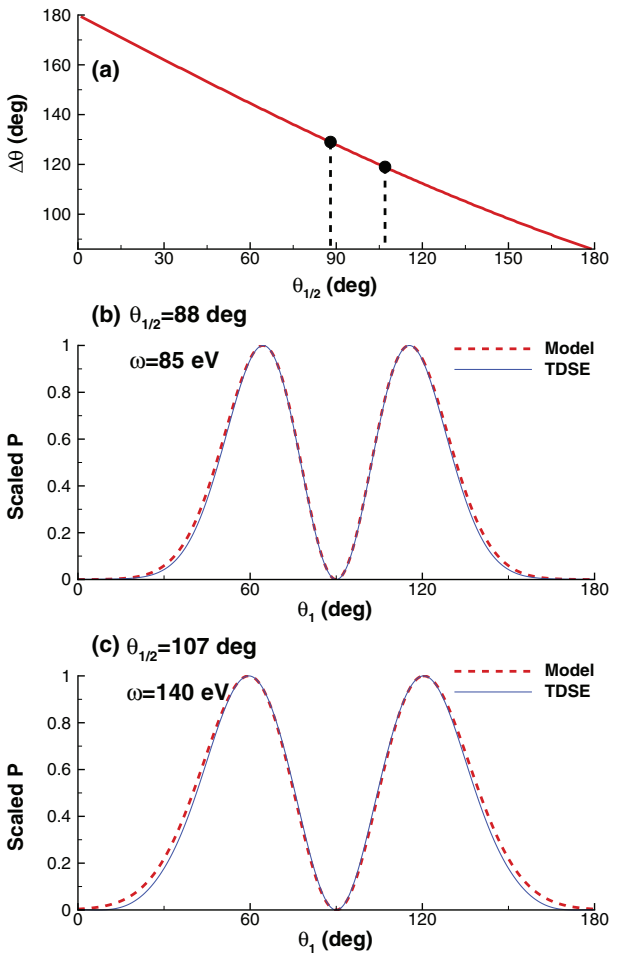

FIG. 3. (Color online) (a) The relation of the interelectron angle $\Delta\theta$ with the fitting parameter $\theta_{1/2}$ built from Eq. (8). (b) and (c): Comparisons of the results according to Eq. (8) and from the TDSE calculations for the one-photon double-ionization process. The photon energy ω and the fitting parameter $\theta_{1/2}$ are marked in the corresponding panel.

exists when the direction of the total momentum of the two electrons is perpendicular to the direction of the laser polarization [10,68], i.e., $\theta_1 + \theta_2 = \pi$ or 3π [see Fig. 1(a2)].

Situations are different for the two-photon double-ionization process. As can be seen from Figs. 1(b1) and 1(c1), for the equal energy sharing case, the back-to-back mode is the most favorable ejection mode for both the sequential and the nonsequential two-photon double-ionization processes [57]. The second forbidden mode for the one-photon process does not exist either in the two-photon process [see Figs. 1(b2) and 1(c2)].

For the one-photon double-ionization process and the two-photon nonsequential double-ionization process, the signals that the two electrons are ejected in exactly the same direction along the laser polarization ($\theta_1 = \theta_2 = 0$ or π) are almost invisible [see Figs. 1(a3) and 1(b3)]. However, such signals in the two-photon sequential double-ionization process are not negligible [Fig. 1(c3)]. We emphasize that, due to the Coulomb repulsion, even this signal will gradually disappear if the radial box size and the waiting time are significantly increased.

B. The interelectron angles $\Delta\theta$ and the electron correlation

Despite those different features in the joint angular distributions discussed in the last subsection, common features do exist in these three types of double ionization processes, i.e., four peaks (marked as A, B, C, and D in the third column of Fig. 1) appear along the line $\theta_1 + \theta_2 = 2\pi$. The ionization signal along this line means that the two electrons are symmetrically ejected with respect to the laser polarization. The peaks A and D (B and C) are just symmetrical peaks by exchanging the two electrons. To be brief, we show only peaks A and B in the following (see Figs. 2 and 3). In addition, the peaks A(C) and B(D) are symmetric peaks for a sufficiently long pulse in which case the carrier envelope phase effects can be neglected. So these four peaks are naturally identical symmetric peaks (see the bottom of Fig. 1), which indicates that the two electrons strongly favor a particular interelectron angle $\Delta\theta$ for the symmetric ejection mode. In the following, we show that such an interelectron angle is closely related to the electron correlation and can well mimic electronic correlation in different double-ionization processes. We note that, such

TABLE I. Comparisons of the fitting parameters $\theta_{1/2}$ between the present TDSE calculations and the experimental results in previous studies.

ω (eV)	$\Delta\theta$ (deg)	$\theta_{1/2}$ (deg)	$\theta_{1/2}$ (deg) from experiments
85	129.0	88	84.7 ± 1.2 [14]
90	128.7	88	87.13 ± 2 for $\omega = 89$ eV [15]
95	128.4	89	91 ± 2 for $\omega = 97.6$ eV [16]
100	127.8	90	91.6 ± 2 [14], 91.0 ± 2 [17], 90.0 ± 3 [21] for $\omega = 99$ eV
105	126.9	92	92 ± 2 for $\omega = 104$ eV [18]
110	125.7	94	
115	124.8	96	
120	123.6	98	103 ± 2 for $\omega = 119$ eV [19]
125	122.4	100	
130	121.2	102	
135	120.0	105	
140	119.0	107	109 ± 2 for $\omega = 139$ eV [20]
160	116.3	112	120 ± 4 for $\omega = 159$ eV [21]

an interelectron angle $\Delta\theta$ has also been recently studied in Ref. [69] for the two-electron attosecond streaking.

The interelectron angle $\Delta\theta$ is extracted from the four peaks by

$$\begin{aligned} &\text{Peak A: } \Delta\theta = 2\theta_1, \\ &\text{Peak B: } \Delta\theta = 2(\pi - \theta_1), \\ &\text{Peak C: } \Delta\theta = 2(\theta_1 - \pi), \\ &\text{Peak D: } \Delta\theta = 2(2\pi - \theta_1). \end{aligned} \tag{7}$$

In our calculations, the differences of the interelectron angles $\Delta\theta$ from each case of the four cases are smaller than 0.3°. In this paper, we take the average value of the four cases as the interelectron angle $\Delta\theta$.

Before giving any further discussions, it is important to make sure that the interelectron angle $\Delta\theta$ is insensitive to the intensity, length, and envelope of the pulse in the perturbation region. In Fig. 2(a), we change the laser peak intensity from 10^{11} to 10^{13} W/cm^2 for the one-photon double-ionization process. We see that the dependence of the interelectron angle $\Delta\theta$ on the intensity is invisible. In Fig. 2(b), the pulse length is varied from 1 to 3 fs for the two-photon nonsequential double-ionization processes. We see that the variation of the interelectron angle $\Delta\theta$ is smaller than 2° and the difference between the 2-fs case and the 3-fs case is almost invisible. In Fig. 2(c), a more realistic Gaussian-shape pulse is compared with the sin-square-shape pulse for the two-photon sequential double-ionization process. The total duration of the Gaussian-shape pulse is taken as four times the full width at half maximum (FWHM) of the Gaussian envelope. The interelectron angle $\Delta\theta$ calculated from the sin-square-shape pulse and the Gaussian-shape pulse is 95° and 93°, respectively. We see that the use of a Gaussian-shape pulse does not significantly change the interelectron angle $\Delta\theta$. These results show that the interelectron angle $\Delta\theta$ is indeed an intrinsic character of a particular ionization process.

The one-photon double-ionization process of helium has been understood quite well in previous studies. A formula based on the Wannier theory [22–24] is widely used to fit the experimental data of the angular distributions of the two ejected electrons. In the equal energy sharing case ($E_1 = E_2$), the dependence of the differential probability density on the ejected angles of the two electrons on the coplane satisfies [10,22,23]

$$P(\theta_1,\theta_2) \propto (\cos\theta_1 + \cos\theta_2)^2 e^{-4\ln 2\left(\frac{\theta_{12}-\pi}{\theta_{1/2}}\right)^2}, \tag{8}$$

where θ_{12} ($0 \leqslant \theta_{12} \leqslant \pi$) is the angle between the two electrons and $\theta_{1/2}$ is a fitting parameter, which stands for the FWHM of the Gaussian-shape envelope centered at π. In fact, all the forbidden lines mentioned in Sec. III A can be understood directly from the factor $(\cos\theta_1 + \cos\theta_2)^2$ in Eq. (8).

It was widely accepted that the parameter $\theta_{1/2}$ can be used to measure the electron correlation [10,19]. It is possible to extract the interelectronic angle $\Delta\theta$ from Eq. (8) using the same strategy that we used for the TDSE result. Therefore we can built a one-to-one correspondence between the interelectron angle $\Delta\theta$ and the fitting parameter $\theta_{1/2}$ [see Fig. 3(a)].

In Figs. 3(b) and 3(c), we adjust the parameter $\theta_{1/2}$ to fit the TDSE results of the one-photon process for $\omega = 85$ and 140 eV. As one can see, the results predicted by Eq. (8) coincide with the TDSE results very well. In Table I, we list the fitting parameters $\theta_{1/2}$ which are suitable for the corresponding photon energies together with some experimental results in the literature. The agreement between our fitting and the experimental results is very satisfactory, except that the discrepancies are slightly larger for $\omega = 85$ eV and 160 eV. The fitting parameters $\theta_{1/2}$ for a series of excess energies have also been given in Ref. [70] theoretically. These comparisons make us confident in the accuracy of our numerical results.

From the above discussions, we can establish a direct connection between $\Delta\theta$ and $\theta_{1/2}$ in Eq. (8). It is clear that the interelectron angle $\Delta\theta$ can play the same role of the parameter $\theta_{1/2}$ to measure the electron correlation strength in the one-photon double ionization. As has been seen, common features exist for the three different kinds of double ionization along the line $\theta_1 + \theta_2 = 2\pi$. This reminds us that the interelectron angle $\Delta\theta$ may reflect the electron correlation strength in all three cases.

Actually, the relation of the interelectron angle $\Delta\theta$ with the electron correlation strength may be understood intuitively in a classical way. In the symmetrical ejection mode considered here, both the positions and the momenta of the two electrons are images which are symmetric to the laser polarization. The electron repulsion only contributes to the electrons'

momentum component which is perpendicular to the laser polarization. Meanwhile, the momentum component of the two electrons along the laser polarization mainly comes from the contribution of the interaction between the laser field and the electrons. Since the interelectron angle $\Delta\theta$ depends on the ratio of the two components of the momentum, one may expect that the stronger the electron correlation is, the larger the interelectron angle $\Delta\theta$ will be.

We have to emphasize that the situation in the two-photon double-ionization process is much more complex than that in the one-photon double ionization. Different from the one-photon case, where only a pure $^1P^o$ final state is excited, the two-photon process involves two kinds of final states, the states with the symmetries $^1S^e$ and $^1D^e$. No simple and accurate fitting equation similar to Eq. (8) exists. Since the interelectron angle $\Delta\theta$, which is closely related to the electron correlation, is the common character in JAD for those double-ionization processes, it is reasonable to treat the interelectronic angle $\Delta\theta$ as a candidate to measure the electron correlation in the three kinds of two-photon double-ionization process. The interelectron angle $\Delta\theta$ is strongly related to the electronic correlation, so it could be a good candidate to measure the electronic correlation in the two-photon double-ionization process.

C. Comparison study of $\Delta\theta$ in different double-ionization processes

In this subsection, we carry out a detailed comparison study of the interelectron angle $\Delta\theta$ in the three different types of double-ionization processes. We show that the interelectron angles $\Delta\theta$ in different ionization processes are obviously different, which means that the electron correlation strengths can be quite different.

We first look at the interelectron angle $\Delta\theta$ as a function of different excess energy E_{exce} for the one-photon and two-photon ($\omega_1 = \omega_2$) double ionization, as shown in Fig. 4(a). For all the calculations, the laser pulses have 15 cycles. For the one-photon double-ionization process, the series of pulses have center frequencies ranging from 85 to 105 eV, which means that the excess energies range from 6 to 26 eV. For the two-photon nonsequential double ionization, the series of pulses have center frequencies ranging from 42.5 to 52.5 eV, which produce the same excess energies as those in the one-photon processes.

We observe that the interelectron angle decreases with the excess of energy in both the one-photon and the two-photon nonsequential double-ionization process. Such an observation has been noticed previously [57]. It is well known that the electron correlation decreases with the excess of energy in the one-photon double-ionization process. If that argument is also true for the two-photon process, then we can conclude that the evolution of the ejection angle mimics that of the electron-electron correlation. Such an observation can also be understood well with the classical picture described in Sec. III B. Since the photon mainly contributes to the electron momentum component along the laser polarization direction, the increase of the photon energy will enlarge the ratio between the momentum component parallel with and perpendicular to the laser polarization, which will decrease the interelectron angle $\Delta\theta$.

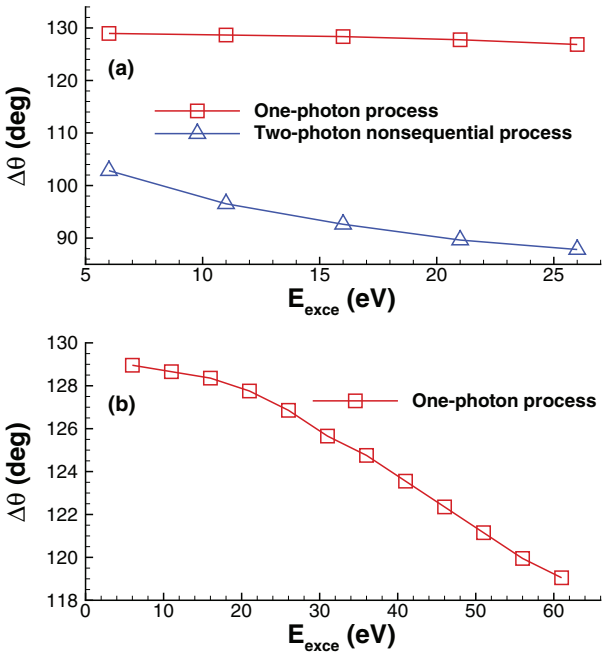

FIG. 4. (Color online) (a) The comparison of the interelectron angles $\Delta\theta$ in the one-photon double-ionization process (squares) and the two-photon nonsequential double-ionization process (triangles) for a series of excess energies. (b) Interelectron angles for a wide range of excess energy are shown for the one-photon process.

From the comparison in Fig. 4(a), for the same excess energy, it is clear that the interelectron angle $\Delta\theta$ in the one-photon process is much larger (25° or more) than that in the two-photon nonsequential process. In the two-photon nonsequential process the two photons are still allowed to be absorbed one by one, while in the one-photon process only one electron can absorb the photon and the two electrons get doubly ejected due to the strong electron correlation. According to this intuitive predication, one may infer that the correlation strength in the one-photon process is much stronger than that in the two-photon nonsequential process. Our observation here supports such a predication and shows that the interelectron angle $\Delta\theta$ indeed mimics the electron correlation.

To see more clearly the decreasing tendency for the one-photon process, we show more data with the excess energy up to 61 eV in Fig. 4(b). One can see that in the low-energy range of 6 eV $\leqslant E_{\text{exce}} \leqslant$ 16 eV, the decreasing of the interelectron angle $\Delta\theta$ is rather slow as the excess energy is increased. However, the decreasing becomes much faster in the higher-energy range when $E_{\text{exce}} \geqslant 20$ eV. This is different from the two-photon nonsequential process shown in Fig. 4(a), where the decrease is rather obvious in the same low-energy range. The different behaviors in the low-energy range and the high-energy range for the one-photon process might come from the competition of the knock-out mechanism which dominates in the low-energy range [71] and the shake-off mechanism which dominates in high-energy range [10,72,73], because quite different electron correlations may be involved in such two ionization mechanisms.

It will be instructive to look at the interelectron angle for the nonsequential and sequential double-ionization processes

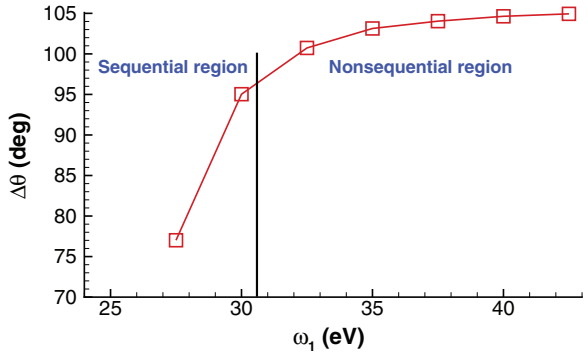

FIG. 5. (Color online) Comparison of the interelectron angle in the two-photon sequential and nonsequential double-ionization processes. The pulse durations are all taken to be 3 fs. The sum of the energies of the two photons are fixed as $\omega_1 + \omega_2 = 85$ eV. The boundary ($\omega_1 = 30.6$ eV) of the sequential and nonsequential regions is marked as a vertical black line.

at a fixed excess energy. In Fig. 5, we show $\Delta\theta$ for double pulses whose envelopes are overlapped with each other and the sum of the central frequency is fixed to be $\omega_1 + \omega_2 = 85$ eV ($\omega_1 \leqslant \omega_2$). Each of the pulses lasts about 3 fs in all the calculations. Note that, in the region of 24.6 eV $< \omega_1 <$ 30.6 eV, the two electrons can be ionized sequentially, while in the region of 30.6 eV $< \omega_1 <$ 42.5 eV the double-ionization process is nonsequential. The boundary of $\omega_1 = 30.6$ eV is marked as a vertical black line in Fig. 5. In the nonsequential region, the interelectron angle $\Delta\theta$ is not sensitive to the ratio of the energies of two photons, indicating that the two electrons are ionized in a quite similar mechanism. By comparing the sequential and nonsequential regions, one easily find that the interelectron angle $\Delta\theta$ in the sequential process is obvious smaller than that in the nonsequential precess, which is exactly what one can expect: in the sequential process, the two electrons can get ionized sequentially, where small electron correlation is involved.

The above observations and discussions agree with our previous knowledge of double-ionization processes and our intuitive expectation of the electron correlation effect, which shows that $\Delta\theta$ can mimic the electron correlation.

IV. CONCLUSION

In conclusion, we have studied the coplanar angular distributions of the two ejected electrons in the equal energy sharing case for one-photon, two-photon nonsequential, and two-photon sequential double-ionization processes. The different and common features of the angular distributions in different processes are discussed. We find that, for the symmetric ejection mode with respect to the laser polarization in all three types of the double-ionization processes, the two electrons always favor a particular interelectron angle, which can mimic electron correlation. We show that this angle in different ionization processes is obviously different even for the same excess energy, which reflects different strengths of the electron correlations in different ionization processes. The interelectron angle is not sensitive to the ratio of the energies of two photons in the two-photon nonsequential double-ionization processes when the excess energy is the same, indicating similar ionization mechanisms. In addition, different behaviors are found when we analyze the dependence of the interelectron angle on the excess energy in the one-photon double-ionization process and the two-photon nonsequential double-ionization process. With the development of the relevant experimental technologies, we hope the future differential measurements may confirm our finding in the present work.

ACKNOWLEDGMENTS

This work is supported by the 973 Program under Grant No. 2013CB922402 and by the National Natural Science Foundation of China under Grants No. 11174016, No. 11121091, and No. 11134001. The computational results were obtained by using the computer cluster "MESO" at the State Key Laboratory for Mesoscopic Physics at Peking University.

[1] D. N. Fittinghoff, P. R. Bolton, B. Chang, and K. C. Kulander, Phys. Rev. Lett. **69**, 2642 (1992).
[2] R. Grobe, K. Rzażewski, and J. H. Eberly, J. Phys. B: At., Mol. Opt. Phys. **27**, L503 (1994).
[3] W.-C. Liu, J. H. Eberly, S. L. Haan, and R. Grobe, Phys. Rev. Lett. **83**, 520 (1999).
[4] C. Figueira de Morisson Faria and X. Liu, J. Mod. Opt. **58**, 1076 (2011).
[5] W. Ackermann *et al.*, Nat. Photonics **1**, 336 (2007).
[6] T. Shintake *et al.*, Nat. Photonics **2**, 555 (2008).
[7] B. McNeil, Nat. Photonics **3**, 375 (2009).
[8] G. Sansone, E. Benedetti, F. Calegari, C. Vozzi, L. Avaldi, R. Flammini, L. Poletto, P. Villoresi, C. Altucci, R. Velotta, S. Stagira, S. De Silverstri, and M. Nisoli, Science **314**, 443 (2006).
[9] E. Goulielmakis, M. Schultze, M. Hofstetter, V. S. Yakovlev, J. Gagnon, M. Uiberacker, A. L. Aquila, E. M. Gullikson, D. T. Atwood, R. Kienberger, F. Krausz, and U. Kleineberg, Science **320**, 1614 (2008).
[10] L. Avaldi and A. Huetz, J. Phys. B: At., Mol. Opt. Phys. **38**, S861 (2005).
[11] J. S. Briggs and V. Schmidt, J. Phys. B: At., Mol. Opt. Phys. **33**, R1 (2000).
[12] A. Huetz and J. Mazeau, Phys. Rev. Lett. **85**, 530 (2000).
[13] A. Knapp *et al.*, Phys. Rev. Lett. **89**, 033004 (2002).
[14] R. Dörner, H. Brauning, J. M. Feagin, V. Mergel, O. Jagutzki, L. Spielberger, T. Vogt, H. Khemliche, M. H. Prior, J. Ullrich, C. L. Cocke, and H. Schmidt-Bocking, Phys. Rev. A **57**, 1074 (1998).
[15] O. Schwarzkopf, B. Krässing, J. Elmiger, and V. Schmidt, Rev. Lett. **70**, 3008 (1993).
[16] L. Malegat, P. Selles, and A. Huetz, J. Phys. B: At., Mol. Opt. Phys. **30**, 251 (1997); L. Malegat, P. Selles, P. Lablanquie, J. Mazeau, and A. Huetz, *ibid.* **30**, 263 (1997).

[17] O. Schwarzkopf, B. Krässing, V. Schmidt, F. Maulbetsch, and J. Briggs, J. Phys. B: At., Mol Opt. Phys. **27**, L347 (1994).
[18] S. A. Collins, A. Huetz, T. J. Reddish, D. P. Seccombe, and K. Soejima, Phys. Rev. A **64**, 062706 (2001).
[19] S. Cvejanović and T. J. Reddish, J. Phys. B: At., Mol. Opt. Phys. **33**, 4691 (2000).
[20] C. Dawson, S. Cvejanović, D. P. Seccombe, T. J. Reddish, F. Maulbetsch, A. Huetz, J. Mazeau, and A. S. Kheifets, J. Phys. B: At., Mol. Opt. Phys. **34**, L525 (2001).
[21] G. Turri, L. Avaldi, P. Bolognesi, R. Camilloni, M. Coreno, J. Berakdar, A. S. Kheifets, and G. Stefani, Phys. Rev. A **65**, 034702 (2002).
[22] A. Huetz, P. Selles, D. Waymel, and J. Mazeau, J. Phys. B: At., Mol. Opt. Phys. **24**, 1917 (1991).
[23] J. M. Feagin, J. Phys. B: At., Mol. Opt. Phys. **17**, 2433 (1984).
[24] G. H. Wannier, Phys. Rev. **90**, 817 (1953).
[25] H. Hasegawa, E. J. Takahashi, Y. Nabekawa, K. L. Ishikawa, and K. Midorikawa, Phys. Rev. A **71**, 023407 (2005).
[26] Y. Nabekawa, H. Hasegawa, E. J. Takahashi, and K. Midorikawa, Phys. Rev. Lett. **94**, 043001 (2005).
[27] A. A. Sorokin, M. Wellhöfer, S. V. Bobashev, K. Tiedtke, and M. Richter, Phys. Rev. A **75**, 051402(R) (2007).
[28] E. Foumouo, H. Bachau, and B. Piraux, Eur. Phys. J.: Spec. Top. **175**, 175 (2009).
[29] X. Guan, K. Bartschat, and B. I. Schneider, Phys. Rev. A **77**, 043421 (2008).
[30] S. X. Hu, J. Colgan, and L. A. Collins, J. Phys. B: At., Mol. Opt. Phys. **38**, L35 (2005).
[31] K. Stefańska, F. Reynal, and H. Bachau, Phys. Rev. A **85**, 053405 (2012).
[32] D. A. Horner, F. Morales, T. N. Rescigno, F. Martín, and C. W. McCurdy, Phys. Rev. A **76**, 030701(R) (2007).
[33] A. Palacios, T. N. Rescigno, and C. W. McCurdy, Phys. Rev. A **79**, 033402 (2009).
[34] A. Palacios, D. A. Horner, T. N. Rescigno, and C. W. McCurdy, J. Phys. B: At., Mol. Opt. Phys. **43**, 194003 (2010).
[35] R. Shakeshaft, Phys. Rev. A **76**, 063405 (2007).
[36] H. Bachau, Phys. Rev. A **83**, 033403 (2011).
[37] J. Feist, S. Nagele, R. Pazourek, E. Persson, B. I. Schneider, L. A. Collins, and J. Burgdörfer, Phys. Rev. A **77**, 043420 (2008).
[38] P. Lambropoulos, L. A. A. Nikolopoulos, M. G. Makris, and A. Mihelič, Phys. Rev. A **78**, 055402 (2008).
[39] J. Colgan and M. S. Pindzola, Phys. Rev. Lett. **88**, 173002 (2002).
[40] M. A. Kornberg and P. Lambropoulos, J. Phys. B: At., Mol. Opt. Phys. **32**, L603 (1999).
[41] L. Malegat, H. Bachau, B. Piraux, and F. Reynal, J. Phys. B: At., Mol. Opt. Phys. **45**, 175601 (2012).
[42] O. Chuluunbaatar, H. Bachau, Y. V. Popov, B. Piraux, and K. Stefańska, Phys. Rev. A **81**, 063424 (2010).
[43] I. A. Ivanov and A. S. Kheifets, Phys. Rev. A **79**, 023409 (2009).
[44] P. Lambropoulos and L. A. Nikolopoulos, New J. Phys. **10**, 025012 (2008).
[45] E. Foumouo, P. Antoine, H. Bachau, and B. Piraux, New J. Phys. **10**, 025017 (2008).
[46] H. Bachau, E. Foumouo, P. Antoine, B. Piraux, O. Chuluunbaatar, Y. Popov, and R. Shakeshaft, J. Phys.: Conf. Ser. **212**, 012001 (2010).
[47] E. Foumouo, G. L. Kamta, G. Edah, and B. Piraux, Phys. Rev. A **74**, 063409 (2006).
[48] H. Ni, S. Chen, C. Ruiz, and A. Becker, J. Phys. B: At., Mol. Opt. Phys. **45**, 049601 (2011).
[49] Y. Qiu, J.-Z. Tang, J. Burgdörfer, and J. Wang, Phys. Rev. A **57**, R1489 (1998).
[50] J. Feist, S. Nagele, R. Pazourek, E. Persson, B. I. Schneider, L. A. Collins, and J. Burgdörfer, Phys. Rev. Lett. **103**, 063002 (2009).
[51] E. Foumouo, P. Antoine, B. Piraux, L. Malegat, B. Bachau, and R. Shakeshaft, J. Phys. B: At., Mol. Opt. Phys. **41**, 051001 (2008).
[52] H. Bachau and P. Lambropoulos, Phys. Rev. A **44**, R9 (1991).
[53] S. Laulan and H. Bachau, Phys. Rev. A **68**, 013409 (2003).
[54] S. Askeland, R. Nepstad, and M. Førre, Phys. Rev. A **85**, 035404 (2012).
[55] S. Fritzsche, A. N. Grum-Grzhimailo, E. V. Gryzlova, and N. M. Kabachnik, J. Phys. B: At., Mol. Opt. Phys. **41**, 165601 (2008).
[56] M. Førre, S. Selstø, and R. Nepstad, Phys. Rev. Lett. **105**, 163001 (2010).
[57] Z. Zhang, L.-Y. Peng, M.-H. Xu, A. F. Starace, T. Morishita, and Q. Gong, Phys. Rev. A **84**, 043409 (2011).
[58] L.-Y. Peng, Z. Zhang, W.-C. Jiang, G.-Q. Zhang, and Q. Gong, Phys. Rev. A **86**, 063401 (2012).
[59] T. N. Rescigno and C. W. McCurdy, Phys. Rev. A **62**, 032706 (2000).
[60] M. J. Rayson, Phys. Rev. E **76**, 026704 (2007).
[61] S. X. Hu and L. A. Collins, Phys. Rev. Lett. **96**, 073004 (2006).
[62] L. Tao, C. W. McCurdy, and T. N. Rescigno, Phys. Rev. A **82**, 023423 (2010).
[63] X. Guan, E. B. Secor, K. Bartschat, and B. I. Schneider, Phys. Rev. A **84**, 033420 (2011).
[64] C. W. McCurdy, M. Baertschy, and T. N. Rescigno, J. Phys. B: At., Mol. Opt. Phys. **37**, R137 (2004).
[65] Y. Saad, *Numerical Methods For Large Eigenvalue Problems* (Halsted, New York, 1992).
[66] L.-Y. Peng and A. F. Starace, J. Chem. Phys. **125**, 154311 (2006).
[67] X.-F. Hou, L.-Y. Peng, Q.-C. Ning, and Q. Gong, J. Phys. B: At., Mol. Opt. Phys. **45**, 074019 (2012).
[68] F. Maulbetsch and J. S. Briggs, J. Phys. B: At., Mol. Opt. Phys. **28**, 551 (1995).
[69] A. Emmanouilidou, A. Staudte, and P. B. Corkum, New J. Phys. **12**, 103024 (2010).
[70] A. S. Kheifets and I. Bray, Phys. Rev. A **62**, 065402 (2000).
[71] J. A. R. Samson, Phys. Rev. Lett. **65**, 2861 (1990).
[72] T. Schneider, P. L. Chocian, and J. M. Rost, Phys. Rev. Lett. **89**, 073002 (2002).
[73] T. Schneider and J. M. Rost, Phys. Rev. A **67**, 062704 (2003).